

# DRED: Deep REDundancy Coding of Speech Using a Rate-Distortion-Optimized Variational Autoencoder

Jean-Marc Valin, *Member, IEEE*, Jan Bütche, *Member, IEEE*, Ahmed Mustafa, Michael Klingbeil

**Abstract**—Despite recent advancements in packet loss concealment (PLC) using deep learning techniques, packet loss remains a significant challenge in real-time speech communication. Redundancy has been used in the past to recover the missing information during losses. However, conventional redundancy techniques are limited in the maximum loss duration they can cover and are often unsuitable for burst packet loss. We propose a new approach based on a rate-distortion-optimized variational autoencoder (RDO-VAE), allowing us to optimize a deep speech compression algorithm for the task of encoding large amounts of redundancy at very low bitrate. The proposed Deep REDundancy (DRED) algorithm can transmit up to 50x redundancy using less than 32 kb/s. Results show that DRED outperforms the existing Opus codec redundancy. We also demonstrate its benefits when operating in the context of WebRTC.

**Index Terms**—neural speech coding, audio redundancy, variational autoencoder

## I. INTRODUCTION

Recent advancements in Deep Packet Loss Concealment (PLC) [1] have demonstrated significant improvements in quality, but also the fundamental limitations of PLC, especially when it comes to intelligibility. For long burst loss, information about missing syllables/words cannot – and should not – be predicted. In parallel, neural speech codecs [2], [3], [4] have also demonstrated their ability to efficiently transmit speech with sufficient quality at very low bitrates and we believe they can play a part in improving how we address packet loss.

One way to improve robustness to lost packets is to transmit redundant information. Some methods, such as RED [5] are generic, whereas the Opus [6] low-bitrate redundancy (LBRR) is specific to that codec. While techniques like LBRR make it possible to transmit redundancy at a somewhat lower bitrate than normal, they cannot scale to large amounts of redundancy without causing impractically large overheads in bitrates.

In this work, we propose adapting recent neural speech coding techniques to the problem of transmitting redundant audio information. The architecture of our Deep REDundancy (DRED) mechanism (Fig. 1) takes advantage of a continuously-operating recurrent encoder with a decoder running backward in time (Section II) to satisfy the unique constraints of redundancy coding. At a lower level, a rate-distortion-optimized variational autoencoder (RDO-VAE) pro-

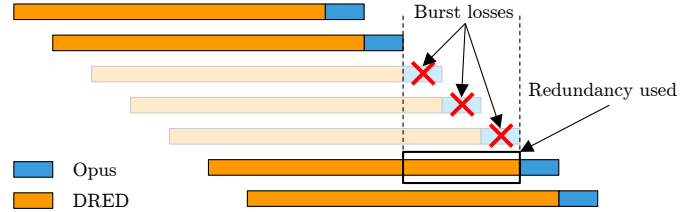


Fig. 1. Illustrating deep redundancy for the case of three consecutive losses. The first packet to arrive after the loss includes enough redundant information to reconstruct the missing audio.

duces a Laplace-distributed latent space that can be quantized efficiently (Section III). We demonstrate (Section IV) that DRED can be used to guard against burst losses up to 1 second (50x redundancy) using less than 32 kb/s, a significant improvement over the Opus LBRR. Results also show that these improvements translate into significant quality improvements in the context of a WebRTC implementation.

This paper is an extended version of [7], including more a detailed description and additional experiments. The algorithm has also been improved with a more efficient encoder-decoder architecture, the addition of rate control to the initial states, and the replacement of the LPCNet vocoder with a new autoregressive vocoder [8], reducing synthesis complexity by a factor of 5. The resulting DRED algorithm is deployed in Opus 1.5, for which we provide an updated evaluation.

## II. DEEP REDUNDANCY (DRED) OVERVIEW

Most speech codecs in use today encode audio in 20-ms frames, with each frame typically being sent in a separate packet over the Internet. When any packet is lost, the corresponding audio is lost and has to be filled by a PLC algorithm. The Opus LBRR option makes it possible for packet number  $n$  to include the contents of both frames  $n$  and  $n - 1$ , with the latter being encoded at a slightly lower bitrate. Effectively, packets each contains 40-ms of audio despite being sent at a 20-ms interval. When LBRR is enabled, a single packet loss does not cause any audio frame to be completely lost, and this can improve the quality in difficult network conditions. Unfortunately, losses are rarely uniformly distributed, and LBRR has limited impact on long loss bursts. While more frames could be coded as part of each packet, it would cause the bitrate to go up significantly. For that reason, we propose an efficient deep speech coding technique that makes it possible to include a large amount of redundancy without a large increase in bitrate.

Jean-Marc Valin and Jan Bütche are with the Xiph.Org Foundation, but the work was conducted while with Amazon Web Services (e-mail: jmvalin@jmvalin.ca, jan.buethe@ieee.org)

Ahmed Mustafa and Michael Klingbeil are with Amazon Web Services (e-mail: ahdmust@amazon.com, klingm@amazon.com).

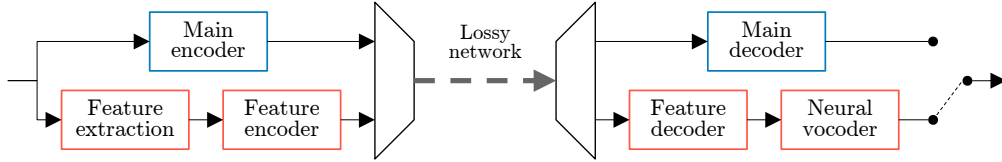


Fig. 2. High-level overview of a communication system using deep redundancy.

The redundancy is encoded separately, but multiplexed with the regular packets during transmission (Fig. 2) in a way that preserves compatibility with the original Opus specification. On the receiver side, it is only used when packets are lost. Although one could design a complete communication system using only the redundancy path, the “legacy” Opus coding still has higher no-loss quality and better handling of non-speech signals. Just like LBRR, DRED is only targeted at speech.

The proposed deep redundancy coding scheme exploits the fact that neural vocoders can generate high-quality speech from low-dimensional acoustic features. For the present application, these are chosen to be 18-Bark frequency cepstral coefficients (BFCC), a pitch period estimated according to [9], and a pitch correlation estimated on the low-passed speech. These features are computed on 20-ms overlapping windows at a 10-ms interval, making it easy to interface with speech communication systems that typically operate with multiples of 10 ms.

The signal-level architecture for the proposed redundancy coding is derived from our previous work on packet loss concealment, where a vocoder is used to fill in the missing frames using acoustic features produced by a predictor (Section 4.3 of [10]). In this work, we replace the acoustic feature predictor by an encoder and decoder that transmit a lossy approximation of the ground-truth features. While [11] proposes coding a prediction residual, we instead project the features onto a latent space to further improve coding efficiency. Although we only discuss redundant audio coding here, our architecture makes it easy to integrate redundancy coding with PLC.

#### A. Constraints and assumptions

Since the purpose of this work is to improve robustness to packet loss, an obvious constraint is to avoid any prediction across different packets. That being said, within each packet, any amount of prediction is allowed since we assume that a packet either arrives uncorrupted, or does not arrive at all. Additionally, since the same frame information is encoded in multiple packets, we do not wish to re-encode each packet *from scratch*, but rather have a continuously-running encoder from which we extract overlapping encoded frames. On the decoder side, since short losses are more likely than very long ones, it is desirable to be able to decode only the last few frames of speech without having to decode the entire packet.

To maximize efficiency, we can take advantage of (variable-length) entropy coding. Even if a constant bitrate was ultimately desired, that could easily be achieved by varying the duration of the redundancy. We can also take advantage of variable encoding quality as a function of the timestamp

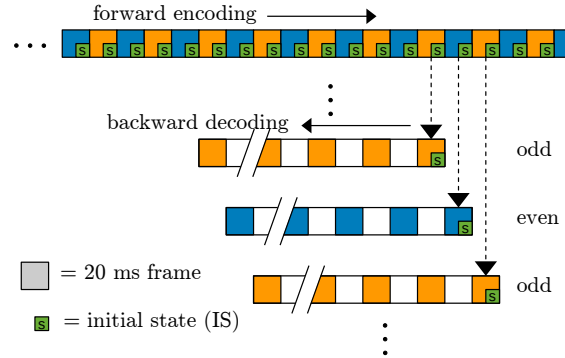


Fig. 3. Overview of the encoding and decoding process. For each 20-ms frame, the encoder processes two 10-ms feature vectors and produces an encoded latent vector (shown in orange or blue), as well as an initial state (IS). Although latent vectors are produced every 20 ms, they each contain sufficient information to reconstruct 40 ms of audio. The encoded stream is *split* into overlapping redundancy packets. Each packet to be sent contains a single IS (for the latest frame), as well as half of the latent vectors (even or odd) spanning the desired redundancy duration.

within the redundant payload. Since more recent redundancy is expected to be used more often, it deserves to be coded at a higher quality.

Although there are many different types of neural vocoders, we propose to use an auto-regressive vocoder, as it allows for seamless transitions between regular coded audio and low-bitrate redundant audio without the use of cross-fading. Although our previous work used LPCNet [12], we use the newer Framewise Autoregressive GAN (FARGAN) [8] vocoder, which has better quality than LPCNet, and about 1/5th of the complexity. FARGAN’s efficiency is achieved by combining framewise generation [13] with a pitch-based autoregressive component [14]. It generates speech one 2.5-ms sub-frame at a time, based on the previous sub-frame as well as an explicit long-term pitch prediction based on the previously synthesized speech. Unlike many other autoregressive vocoders, it is trained in closed loop (unrolling the network) without the use of teacher forcing. FARGAN is conditioned on the same 10-ms frame features as LPCNet.

#### B. Proposed architecture

There are generally two methods for improving coding efficiency: prediction and transforms. The proposed algorithm leverages both methods. In the context of neural coding, grouping input feature vectors together enables the encoder to infer an efficient non-linear transform of its input. For prediction, we use a recurrent neural network (RNN) architecture, but

to achieve the computational goals listed above, we make the encoder RNN run forward in a continuous manner, while making the decoder RNN run backward in time from the most recent packet encoded. Since the process is analogous to delta coding, the encoder also codes an *initial state* (IS) to ensure that the decoder achieves sufficient quality on the first (most recent) packet. The IS vector contains the most recent information and is used to initialize the decoder. Although the encoder needs to produce such an IS on every frame, only one (the most recent) is included in each redundancy packet.

Even though our network operates on 20-ms frames, the underlying 20-dimensional acoustic feature vectors are computed on a 10-ms interval. For that reason we group feature vectors in pairs – equivalent to a 20-ms non-linear transform. To further increase the effective transform size while still producing a redundancy packet every 20 ms, we use an output stride. The process is illustrated for a stride of 2 in Fig. 3 – resulting in each output vector representing 40 ms of speech – but it can easily scale to larger strides.

### III. RATE-DISTORTION-OPTIMIZED VAE

As stated above, our goal is to compress each redundancy packet as efficiently as possible. Although VQ-VAE [15] has been a popular choice for deep speech coding [16], [17], in this work we avoid its large fixed-size codebooks and investigate other variational auto-encoders (VAE) [18]. Our approach is instead inspired from recent work in VAE-based image coding [19], [20] combining scalar quantization with entropy coding.

We propose a rate-distortion-optimized VAE (RDO-VAE) that directly minimizes a rate-distortion loss function. From a sequence of input vectors  $\mathbf{x} \in \mathbb{R}^L$ , the RDO-VAE produces an output  $\tilde{\mathbf{x}} \in \mathbb{R}^L$  by going through a sequence of quantized latent vectors  $\mathbf{z}_q \in \mathbb{Z}^M$ , minimizing the loss function

$$\mathcal{L} = D(\tilde{\mathbf{x}}, \mathbf{x}) + \lambda H(\mathbf{z}_q), \quad (1)$$

where  $D(\cdot, \cdot)$  is the distortion loss, and  $H(\cdot)$  denotes the entropy. The Lagrange multiplier  $\lambda$  effectively controls the target rate, with a higher value leading to a lower rate. The high-level encoding and decoding process is illustrated in Fig. 4.

Because the latent vectors  $\mathbf{z}_q$  are quantized, neither  $D(\cdot, \cdot)$  nor  $H(\cdot)$  in (1) are differentiable. For the distortion, a common way around the problem is to use the *straight-through* estimator [15], [21]. More recently, various combinations involving “soft” quantization – through the addition of uniformly distributed noise – have been shown to produce better results [19], [20]. In this work, we choose to use a weighted average of the soft and straight-through (hard quantization) distortions, as discussed in Sec. III-D and illustrated in Fig. 6.

#### A. Rate estimator

We use the Laplace distribution to model the latent space because it is easy to manipulate and is relatively robust to probability modeling mismatches. Since we can consider the rate of each variable independently, let  $z_e$  and  $z_q$  represent one

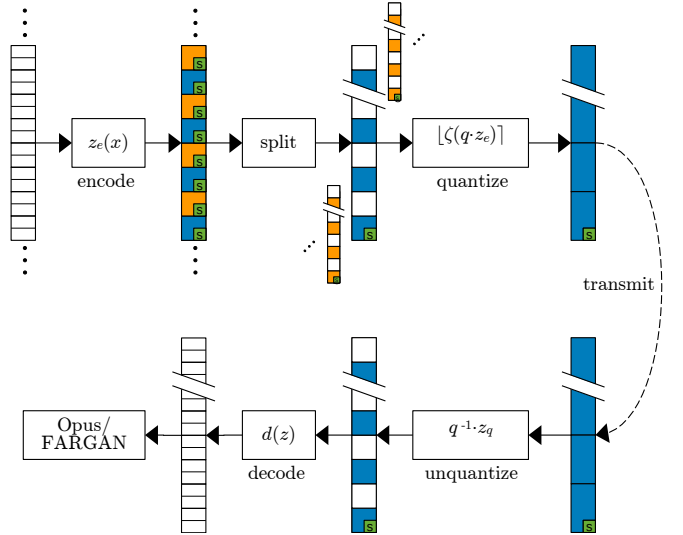


Fig. 4. Encoding and decoding process. The encoder produces latent vectors and initial states from acoustic features. The vectors are split into overlapping redundancy packets and then quantized using a variable resolution (the same vector can be quantized at different rates depending on its position). At the receiver, the redundancy packets are entropy-decoded and scaled back (unquantized) to recover the latent vectors. Those are then decoded to produce 10-ms acoustic feature vectors that can be used to synthesize audio in place of the missing Opus packets. The redundancy decoding process happens only on-demand such that no computation occurs when there is no loss.

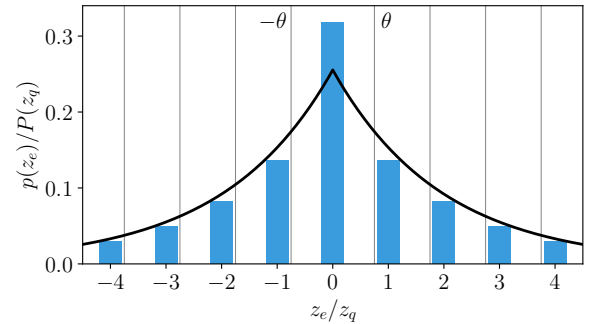


Fig. 5. Continuous Laplace distribution  $p(z_e)$  in black line and the corresponding discrete distribution  $P(z_q)$  in blue solid bars, for  $r = 0.6$  and  $\theta = 0.75$ . The quantization thresholds are shown as gray vertical lines. Note that the reconstruction values are still integers and are not affected by  $\theta$ .

component of the unquantized ( $\mathbf{z}_e$ ) and quantized ( $\mathbf{z}_q$ ) vectors, respectively. The continuous Laplace distribution is given by:

$$p(z_e) = -\frac{\log r}{2} r^{|z_e|}, \quad (2)$$

where  $r$  is related to the standard deviation  $\sigma$  by  $r = e^{-\sqrt{2}/\sigma}$ .

An efficient way of quantizing a Laplace-distributed variable [22] is to use a fixed quantization step size, except around zero, where all values of  $z_e \in ]-\theta, \theta[$  quantize to zero, with  $\theta > \frac{1}{2}$  arising from rate-distortion optimization. We describe a quantizer with a step size of one without loss of generality, since we can always scale the input and output to achieve the desired quantization resolution. We thus define the quantizer as:

$$z_q = Q_\theta(z_e) = \text{sgn}(z_e) [\max(|z_e| + 1 - \theta, 0)], \quad (3)$$

where  $\text{sgn}(\cdot)$  denotes the sign function. In the special case  $\theta = 1/2$ , we simply round to the nearest integer (ignoring ties).

We refer to the distribution of  $z_q$  as the discrete Laplace distribution (Fig. 5)

$$P(z_q) = \begin{cases} 1 - r^\theta & z_q = 0 \\ \frac{1}{2}(1 - r)r^{|z_q| + \theta - 1} & z_q \neq 0 \end{cases}. \quad (4)$$

Since its entropy,  $H(z_q) = \mathbb{E}[-\log_2 P(z_q)]$ , is not differentiable with respect to  $z_e$ , we must find a way to backpropagate the gradient. We find that using the straight-through estimator for the rate results in very poor convergence, with the training loss starting to increase again after a few epochs due to the mismatch between the forward and backward pass of backpropagation.

We seek to use a differentiable rate estimation on the unquantized encoder output. An obvious choice is to use the differential entropy  $h(z_e) = \mathbb{E}[-\log_2 p(z_e)]$ , which achieves better convergence. Unfortunately, the differential entropy tends towards  $-\infty$  when  $p(z_e)$  becomes degenerate as  $r \rightarrow 0$ , which can cause many low-variance latent variables to collapse to zero. Instead, we directly evaluate the entropy of the discrete distribution  $H(z_e) = \mathbb{E}[-\log_2 P(z_e)]$  using the continuous latent  $z_e$ . To avoid the special case around  $z_e = 0$ , we use a value for  $\theta$  for which both cases of (4) are equal for  $z_e = 0$ :

$$1 - r^\theta = \frac{1}{2}(1 - r)r^{\theta - 1} \quad (5)$$

$$\theta = \log_r(2r/(1 + r)). \quad (6)$$

Using the value of  $\theta$  given by (6) results in the generalized discrete entropy

$$H(z_e) = -\log_2 \frac{1 - r}{1 + r} - \mathbb{E}[|z_e|] \log_2 r. \quad (7)$$

which has a form similar to an  $L_1$  loss, but with a penalty term  $-\log_2 \frac{1 - r}{1 + r}$  that counteracts the weighting factor  $\log_2 r$ . In the degenerate case where  $r \rightarrow 0$  (and thus  $z_e = 0$ ), we have  $H(z_e) = 0$ , which is the desired behavior. An advantage of using (7) is that any latent dimension that does not sufficiently reduce the distortion to be “worth” its rate naturally becomes degenerate during training. We can thus start with more latent dimensions than needed and let the model decide on the number of useful dimensions. In practice, we find that different values of  $\lambda$  result in a different number of non-degenerate pdfs (Fig. 7).

### B. Quantization and encoding

The dead zone, as defined by the quantizer  $Q_\theta(z)$  in (3), needs to be differentiable with respect to both its input parameter  $z$  and its width  $\theta$ . That can be achieved by implementing it as the differentiable function

$$\zeta(z) = z - \delta \tanh \frac{z}{\delta + \epsilon}, \quad (8)$$

where  $\delta \approx \theta - 1/2$  controls the width of the dead zone and  $\epsilon = 0.1$  avoids training instabilities. The complete quantization process thus becomes

$$z_q = \lfloor \zeta(q_\lambda \cdot z_e) \rfloor, \quad (9)$$

where  $\lfloor \cdot \rfloor$  denotes rounding to the nearest integer, and  $q_\lambda$  is the quantizer scale (higher  $q_\lambda$  leads to higher quality). The quantizer scale  $q_\lambda$  is learned independently as an embedding matrix for each dimension of the latent space and for each value of the rate-control parameter  $\lambda$ .

The quantized latent components  $z_q$  can be entropy-coded [23] using the discrete pdf in (4) parameterized by  $r$  and  $\theta$ . The value of  $\theta$  is learned independently of the quantizer dead-zone parameter  $\delta$ . Also, we learn a different  $r$  parameter for the soft and hard quantizers. The value of  $\theta$  for the soft quantizer is implicit and thus does not need to be learned, although a learned  $\theta$  does not lead to significant rate reduction, which is evidence that the implicit  $\theta$  is close to the RD-optimal choice.

On the decoder side, the quantized latent vectors are entropy-decoded and the scaling is undone:

$$z_d = q_\lambda^{-1} \cdot z_q. \quad (10)$$

Finally, we need to quantize the IS vector  $\mathbf{s}$  to be used by the decoder. Although the encoder produces an IS at every frame, only one IS per redundancy packet needs to be transmitted. In previous work [7], we used a fixed-bitrate pyramid vector quantizer (PVQ) [24] to transmit the IS vectors since it made training simpler (only one rate). However, not being able to optimize the bitrate as a function of  $\lambda$  is sub-optimal so we instead propose also using RDO-VAE for the IS. We can use the same process as for encoding the latent vectors, with the exception that the rate must be considered differently since only one IS is transmitted for multiple latent vectors. Using the variable rate IS allows the proposed redundancy mechanism to scale to a wider range of bitrates than our previous work.

### C. Encoder and decoder

The encoder and decoder are constructed from a combination of gated recurrent unit (GRU) [25] and 1D convolutional layers in time. To help with gradient propagation and avoid the vanishing gradient problem, we introduce skip connections arranged like in the DenseNet [26] architecture. The encoder and decoder networks each include 5 GRU layers alternating with 5 convolutional layers. We found that the proposed DNN architecture with about 1 million weights for each of the encoder and decoder achieves similar results to the architecture of our previous work that used 2 million weights for each (not considering the other improvements).

### D. Training

During training, we vary  $\lambda$  in such a way as to obtain average rates between 8 and 80 bits per vector. We split the  $\lambda$  range into 16 equally-spaced intervals in the log domain. For each interval, we learn independent values for  $q$ ,  $\delta$ ,  $\theta$ , as well as for the hard and soft versions of the Laplace parameter  $r$ . To avoid giving too much weight to the low-bitrate cases because of the large  $\lambda$  values, we reduce the difference in losses by weighting the total loss values by  $1/\sqrt{\lambda}$ :

$$\mathcal{L} = \frac{D(\tilde{\mathbf{x}}, \mathbf{x})}{\sqrt{\lambda}} + \sqrt{\lambda} \sum_{i=0}^{M-1} H(z_e^{(i)}; r_s^{(i)}). \quad (11)$$

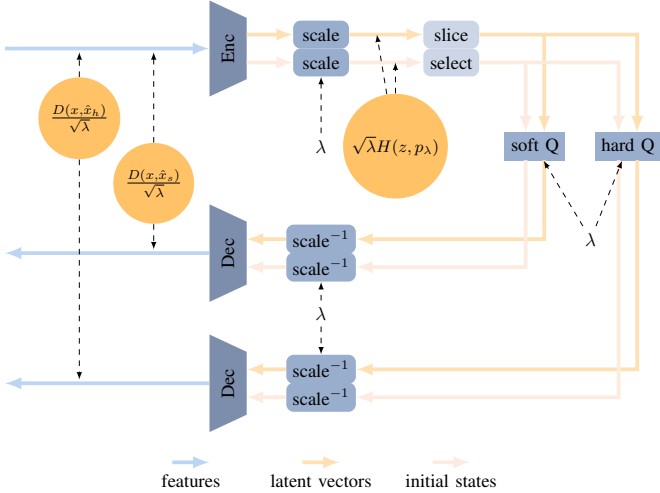


Fig. 6. Setup for training RDO-VAE. Features are encoded by the encoder to produce a sequence of latent vectors and initial states. In *slice* a sub-sequence is sliced from the sequence of latent vectors and in *select* the matching initial state is selected. Initial state and latent vectors are passed both through a hard quantization and a soft quantization unit and the outputs of both units are decoded separately.

The acoustic vector  $\mathbf{x} = [\mathbf{c}, p, v]$  includes an 18-dimensional cepstrum  $\mathbf{c}$ , the log pitch frequency  $f_0$  and the voicing (pitch correlation) parameter  $v$ . The distortion is then defined as

$$D(\tilde{\mathbf{x}}, \mathbf{x}) = E \left[ \|\tilde{\mathbf{c}} - \mathbf{c}\|^2 + w_p |p - \tilde{p}| + |v - \tilde{v}|^2 \right] \quad (12)$$

where the pitch distortion weighting  $w_p = 10v^2$  ensures that we only consider the pitch error for voiced signals.

The large overlap between decoded sequences poses a challenge for the training. Running a large number of overlapping decoders would be computationally challenging. On the other hand, we find that decoding the entire sequence produced by the encoder with a single decoder leads to the model over-fitting to that particular case. We find that encoding 4-second sequences and randomly splitting them into four non-overlapping sequences to be independently decoded leads to acceptable performance and training time. From there, we can ensure robustness to longer sequences by iteratively lengthening the encoded sequences, while maintaining a one-second average decoding duration. The whole training setup is depicted in Fig. 6.

#### IV. EXPERIMENTS & RESULTS

Both the RDO-VAE and the FARGAN vocoder are trained independently on 205 hours of 16-kHz speech from a combination of TTS datasets [27], [28], [29], [30], [31], [32], [33], [34], [35] including more than 900 speakers in 34 languages and dialects. The vocoder training is performed as described in [8].

We train the RDO-VAE with  $M = 80$  initial latent dimensions and observe that, depending on the quantizer, between 4 and 21 dimensions are ultimately non-degenerate (Fig. 7). At the highest bitrate (quantizer 0), the latent vectors are coded with an average of 72 bits each (equivalent to 1.8 kb/s), with 105 bits per IS. At the lowest bitrate (quantizer 15), the latent

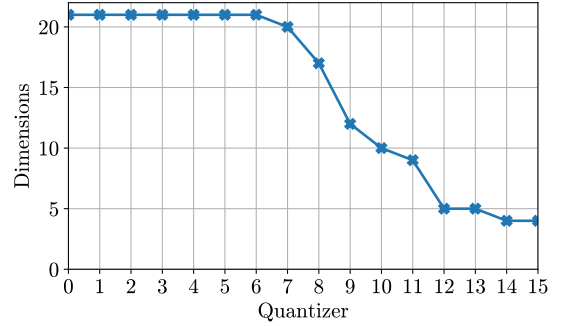


Fig. 7. Number of non-degenerate dimensions for all 16 quantizers, where quantizer 0 corresponds to the highest bitrate and quantizer 15 corresponds to the lowest bitrate.

vectors use just 6 bits (equivalent to 150 b/s), with 48 bits per IS.

We evaluate the proposed deep redundancy mechanism on speech compressed with the Opus codec at 24 kb/s. We add 1.04 seconds of deep redundancy in each 20-ms frame transmitted, so that 52 copies of every frame are ultimately transmitted (concealing burst losses up to 1.02 seconds). We vary the rate within each redundancy packet such that the average rates are around 1250 b/s for the most recent frame and 150 b/s for the oldest. The average rate over all frames is about 650 b/s, including the IS, or 32 kb/s of total redundancy.

A real-time C implementation of DRED operating within the Opus codec (including the FARGAN vocoder) is available under an open-source license<sup>1</sup>. The results correspond to the code released as part of Opus version 1.5<sup>2</sup>.

##### A. Complexity

The DRED encoder and decoder each have about 1 million weights. The encoder uses each weight once (multiply-add) for each 20-ms frame, resulting in a complexity of 100 MFLOPS. The decoder's complexity varies depending on the loss pattern, but it can never decode more than one latent vector every 40 ms on average. That results in a worst-case average decoder complexity of 50 MFLOPS. Unlike the case of the encoder, the decoder complexity can have bursts. On the receiver side, the complexity is dominated by the FARGAN vocoder's 600 MFLOPS worst-case complexity.

##### B. Quality

We evaluated DRED on the PLC Challenge dataset [1], using the development test set files for both the audio and the recorded packet loss sequences (18.4% average loss rate). The sequences have losses ranging from 20 ms to bursts of up to one second, meaning that the redundancy is able to cover all losses without the need for regular PLC. We compare with the deep PLC results obtained in [10] (no redundancy), as well as with the original Opus LBRR<sup>3</sup>, both alone (requiring PLC)

<sup>1</sup>[https://gitlab.xiph.org/xiph/opus/-/tree/jstsp\\_dred/dnn/torch/rdovae](https://gitlab.xiph.org/xiph/opus/-/tree/jstsp_dred/dnn/torch/rdovae)

<sup>2</sup>Demo samples provided at <https://www.opus-codec.org/demo/opus-1.5/>

<sup>3</sup>The total bitrate is increased to 40 kb/s to make room for LBRR, which averages about 16 kb/s.

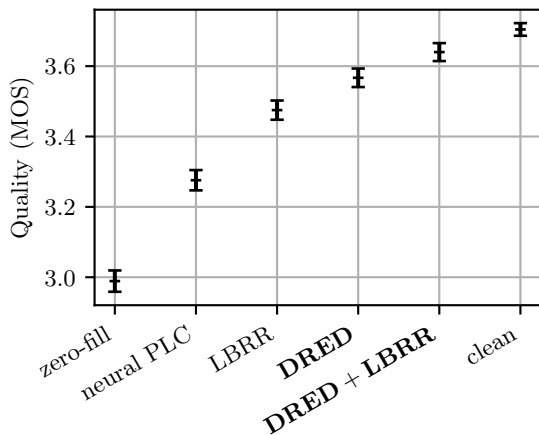


Fig. 8. MOS results, including the 95% confidence intervals. All differences are statistically significant ( $p < .05$ ).

and combined with DRED (the first DRED frame becomes unused). We also include an upper bound where DRED is applied with uncompressed features. We include as anchors both clean/lossless samples and samples where losses are replaced with zeros.

The mean opinion score (MOS) [36] results in Fig. 8 were obtained using the crowdsourcing methodology described in P.808 [37], [38], where each of the 966 test utterances was randomly assigned and evaluated by 10 naive listeners (not all utterances were rated by the same 10 listeners). Listeners were asked to rate samples on an absolute category rating scale from 1 (bad) to 5 (excellent). The results show that DRED significantly outperforms both deep PLC and the existing Opus LBRR. Despite the very low bitrate used for the redundancy, the performance is already close to the uncompressed upper bound, suggesting that the vocoder may already be the performance bottleneck. We also note that LBRR and DRED appear to be complementary, with LBRR being more efficient for short losses and DRED handling long losses.

### C. Complete system

Since Opus is the mandatory-to-implement audio codec for the WebRTC standard [39], we evaluate DRED as part of a complete real-time speech communications system. We modify the `webrtc.org` implementation to add DRED support<sup>4</sup>. That evaluation includes not only the effect of the codec and redundancy, but also the interaction with the jitter buffer. In practice when losses occur, the jitter buffer increases the delay in a similar way to the case where packets arrive later. From the jitter buffer’s point of view, a new DRED-containing packet arriving after a loss can be viewed in the same way as the simultaneous arrival of all the lost packets.

For evaluation, we select a random subset of 200 samples from the dataset used in Sec. IV-B. We generate a single packet loss pattern per-item using a generative model<sup>5</sup> trained from the real loss traces used in Sec. IV-B and conditioned on the

<sup>4</sup><https://github.com/xiph/webrtc-opus-ng/tree/opus-ng>

<sup>5</sup><https://gitlab.xiph.org/xiph/opus/-/blob/main/dnn/lossgen.c>

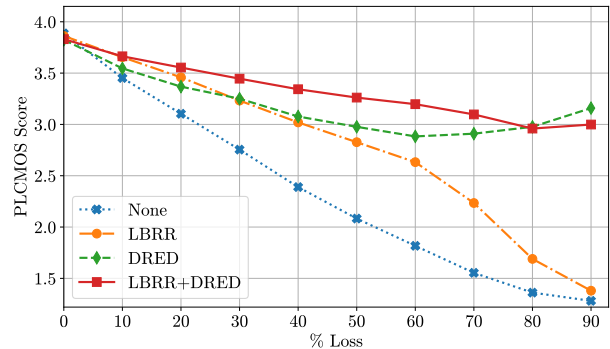


Fig. 9. PLCMOSv2 objective evaluation of the different algorithms as a function of the rate of packet loss.

average loss. We perform objective testing using version 2 of the reference-free PLCMOS<sup>6</sup> algorithm [40]. Results in Fig. 9 also demonstrate the effectiveness of DRED when compared to LBRR or PLC alone.

## V. CONCLUSION

We demonstrate the feasibility and benefits of transmitting large amounts of low-bitrate audio redundancy to improve the robustness of speech communication under burst packet loss. The proposed DRED solution makes use of a rate-distortion-optimized VAE operating in a forward-backward configuration to compute and quantize a sequence of latent vectors at a 40-ms interval and transmit self-contained overlapping segments of redundancy to the receiver. We not only show that DRED is more effective than the Opus LBRR redundancy for high loss rates, but that the two redundancy methods are complementary. Taking advantage of the proposed DRED requires an adaptive jitter buffer. Even though the optimal trade-offs between loss robustness and jitter buffer delay is still an open question, our results in the context of WebRTC demonstrates the practical effectiveness of DRED. The proposed deep redundancy is currently being standardized at the IETF [41] as an extension of the Opus codec.

## REFERENCES

- [1] L. Diener, S. Sootla, S. Branets, A. Saabas, R. Aichner, and R. Cutler, “INTER\_SPEECH 2022 audio deep packet loss concealment challenge,” in *Proc. INTER\_SPEECH*, 2022.
- [2] W. B. Kleijn, F. SC Lim, A. Luebs, J. Skoglund, F. Stimberg, Q. Wang, and T. C. Walters, “WaveNet based low rate speech coding,” in *Proc. International Conference on Acoustics, Speech and Signal Processing (ICASSP)*, 2018, pp. 676–680.
- [3] J. Klejsa, P. Hedelin, C. Zhou, R. Fejgin, and L. Villemoes, “High-quality speech coding with SampleRNN,” in *Proc. International Conference on Acoustics, Speech and Signal Processing (ICASSP)*, 2019.
- [4] J.-M. Valin and J. Skoglund, “A real-time wideband neural vocoder at 1.6 kb/s using LPCNet,” in *Proc. INTER\_SPEECH*, 2019.
- [5] I. Kouvelas, O. Hodson, V. Hardman, M. Handley, J.C. Bolot, A. Vega-Garcia, and S. Fosse-Parisis, “RTP payload for redundant audio data,” RFC 2198, Sept. 1997, <https://tools.ietf.org/html/rfc2198>.
- [6] J.-M. Valin, K. Vos, and T. B. Terriberry, “Definition of the Opus Audio Codec,” RFC 6716, Sept. 2012, <https://tools.ietf.org/html/rfc6716>.

<sup>6</sup><https://github.com/microsoft/PLC-Challenge/tree/main/PLCMOS>

- [7] J.-M. Valin, J. Bütche, and A. Mustafa, “Low-bitrate redundancy coding of speech using a rate-distortion-optimized variational autoencoder,” in *Proc. International Conference on Acoustics, Speech and Signal Processing (ICASSP)*, 2023.
- [8] J.-M. Valin, A. Mustafa, and J. Bütche, “Very low complexity speech synthesis using framewise autoregressive GAN (FARGAN) with pitch prediction,” to appear in *IEEE Signal Processing Letters*, arxiv:2405.21069, 2024.
- [9] K. Subramani, J.-M. Valin, J. Buthe, P. Smaragdis, and M.M. Goodwin, “Noise-robust DSP-assisted neural pitch estimation with very low complexity,” in *Proc. International Conference on Acoustics, Speech and Signal Processing (ICASSP)*, 2024.
- [10] J.-M. Valin, A. Mustafa, C. Montgomery, T.B. Terriberry, M. Klingbeil, P. Smaragdis, and A. Krishnaswamy, “Real-time packet loss concealment with mixed generative and predictive model,” in *Proc. INTERSPEECH*, 2022.
- [11] H. Yang, W. Lim, and M. Kim, “Neural feature predictor and discriminative residual coding for low-bitrate speech coding,” in *Proc. International Conference on Acoustics, Speech and Signal Processing (ICASSP)*, 2023, pp. 1–5.
- [12] J.-M. Valin and J. Skoglund, “LPCNet: Improving neural speech synthesis through linear prediction,” in *Proc. International Conference on Acoustics, Speech and Signal Processing (ICASSP)*, 2019, pp. 5891–5895.
- [13] A. Mustafa, J.-M. Valin, J. Bütche, P. Smaragdis, and M. M. Goodwin, “Framewise wavegan: High speed adversarial vocoder in time domain with very low computational complexity,” in *Proc. International Conference on Acoustics, Speech and Signal Processing (ICASSP)*, 2023.
- [14] M. Morrison, R. Kumar, K. Kumar, P. Seetharaman, A. Courville, and Y. Bengio, “Chunked autoregressive gan for conditional waveform synthesis,” in *Proc. International Conference on Learning Representations (ICLR)*, 2021.
- [15] A. van den Oord, O. Vinyals, and K. Kavukcuoglu, “Neural discrete representation learning,” *Advances in neural information processing systems*, vol. 30, 2017.
- [16] N. Zeghidour, A. Luebs, A. Omran, J. Skoglund, and M. Tagliasacchi, “SoundStream: An end-to-end neural audio codec,” *Trans. on Acoustics, Speech, and Signal Processing*, vol. 30, 2021.
- [17] J. Casebeer, V. Vale, U. Isik, J.-M. Valin, R. Giri, and A. Krishnaswamy, “Enhancing into the codec: Noise robust speech coding with vector-quantized autoencoders,” in *Proc. International Conference on Acoustics, Speech and Signal Processing (ICASSP)*, 2021.
- [18] D.P. Kingma and M. Welling, “Auto-encoding variational Bayes,” arxiv:1312.6114, 2013.
- [19] Z. Guo, Z. Zhang, R. Feng, and Z. Chen, “Soft then hard: Rethinking the quantization in neural image compression,” in *Proc. ICML*, 2021.
- [20] J. Ballé, P. A. Chou, D. Minnen, S. Singh, N. Johnston, E. Agustsson, S.J. Hwang, and G. Toderici, “Nonlinear transform coding,” *IEEE Journal of Selected Topics in Signal Processing*, vol. 15, no. 2, 2021.
- [21] Y. Bengio, N. Léonard, and A. Courville, “Estimating or propagating gradients through stochastic neurons for conditional computation,” arxiv preprint arXiv:1308.3432, 2013.
- [22] G.J. Sullivan, “Efficient scalar quantization of exponential and laplacian random variables,” *IEEE Transactions on Information Theory*, vol. 42, no. 5, 1996.
- [23] G. Nigel and N. Martin, “Range encoding: An algorithm for removing redundancy from a digitised message,” in *Proc. Video and Data Recording Conference*, 1979.
- [24] T. Fischer, “A pyramid vector quantizer,” *IEEE Trans. on Information Theory*, 1986.
- [25] K. Cho, B. Van Merriënboer, D. Bahdanau, and Y. Bengio, “On the properties of neural machine translation: Encoder-decoder approaches,” in *Proceedings of Eighth Workshop on Syntax, Semantics and Structure in Statistical Translation*, 2014.
- [26] G. Huang, Z. Liu, L. Van Der Maaten, and K.Q. Weinberger, “Densely connected convolutional networks,” in *Proceedings of the IEEE conference on computer vision and pattern recognition*, 2017, pp. 4700–4708.
- [27] I. Demirsahin, O. Kjartansson, A. Gutkin, and C. Rivera, “Open-source Multi-speaker Corpora of the English Accents in the British Isles,” in *Proc. LREC*, 2020.
- [28] O. Kjartansson, A. Gutkin, A. Butryna, I. Demirsahin, and C. Rivera, “Open-Source High Quality Speech Datasets for Basque, Catalan and Galician,” in *Proc. SLTU and CCURL*, 2020.
- [29] K. Sodimana, K. Pipatsrisawat, L. Ha, M. Jansche, O. Kjartansson, P. De Silva, and S. Sarin, “A Step-by-Step Process for Building TTS Voices Using Open Source Data and Framework for Bangla, Javanese, Khmer, Nepali, Sinhala, and Sundanese,” in *Proc. SLTU*, 2018.
- [30] A. Guevara-Rukoz, I. Demirsahin, F. He, S.-H. C. Chu, S. Sarin, K. Pipatsrisawat, A. Gutkin, A. Butryna, and O. Kjartansson, “Crowdsourcing Latin American Spanish for Low-Resource Text-to-Speech,” in *Proc. LREC*, 2020.
- [31] F. He, S.-H. C. Chu, O. Kjartansson, C. Rivera, A. Katanova, A. Gutkin, I. Demirsahin, C. Johnny, M. Jansche, S. Sarin, and K. Pipatsrisawat, “Open-source Multi-speaker Speech Corpora for Building Gujarati, Kannada, Malayalam, Marathi, Tamil and Telugu Speech Synthesis Systems,” in *Proc. LREC*, 2020.
- [32] Y. M. Oo, T. Wattanavekin, C. Li, P. De Silva, S. Sarin, K. Pipatsrisawat, M. Jansche, O. Kjartansson, and A. Gutkin, “Burmese Speech Corpus, Finite-State Text Normalization and Pronunciation Grammars with an Application to Text-to-Speech,” in *Proc. LREC*, 2020.
- [33] D. van Niekerk, C. van Heerden, M. Davel, N. Kleynhans, O. Kjartansson, M. Jansche, and L. Ha, “Rapid development of TTS corpora for four South African languages,” in *Proc. INTERSPEECH*, 2017.
- [34] A. Gutkin, I. Demirsahin, O. Kjartansson, C. Rivera, and K. Tübbösün, “Developing an Open-Source Corpus of Yoruba Speech,” in *Proc. INTERSPEECH*, 2020.
- [35] E. Bakhturina, V. Lavrukhin, B. Ginsburg, and Y. Zhang, “Hi-Fi Multi-Speaker English TTS Dataset,” arXiv preprint arXiv:2104.01497, 2021.
- [36] ITU-T, *Recommendation P.800: Methods for subjective determination of transmission quality*, 1996.
- [37] ITU-T, *Recommendation P.808: Subjective evaluation of speech quality with a crowdsourcing approach*, 2018.
- [38] B. Naderi and R. Cutler, “An open source implementation of ITU-T recommendation P.808 with validation,” in *Proc. INTERSPEECH*, 2020.
- [39] J.-M. Valin and C. Bran, “WebRTC audio codec and processing requirements,” RFC 7874, May 2016, <https://tools.ietf.org/html/rfc7874>.
- [40] L. Diener, M. Purin, S. Sootla, A. Saabas, R. Aichner, and R. Cutler, “PLCMOS – a data-driven non-intrusive metric for the evaluation of packet loss concealment algorithms,” in *Proc. INTERSPEECH*, 2023.
- [41] J.-M. Valin and J. Bütche, “Deep audio redundancy (DRED) extension for the opus codec,” draft-ietf-mlcodec-opus-dred, 2024, <https://datatracker.ietf.org/doc/draft-ietf-mlcodec-opus-dred/>.